Adaptive Three-phase Estimation of Sequence Components and Frequency Using H_∞ Filter Based on Sparse Model

Umamani Subudhi, Harish Kumar Sahoo, and Sanjeev Kumar Mishra

***Abstract*—The estimation of sequence or symmetrical components and frequency in three-phase unbalanced power system is of great importance for protection and relay. This paper proposes a new H_∞ filter based on sparse model to track the sequence components and the frequency of three-phase unbalanced power systems. The inclusion of sparsity improves the error convergence behavior of estimation model and hence short-duration non-stationary PQ events can easily be tracked in the time domain. The proposed model is developed using l_1 norm penalty in the cost function of H_∞ filter, which is quite suitable for estimation across all the three phases of an unbalanced system. This model uses real state space modeling across three phases to estimate amplitude and phase parameters of sequence components. However, frequency estimation uses complex state space modeling and Clarke transformation generates a complex measurement signal from the unbalanced three-phase voltages. The state vector used for frequency estimation consists of two state variables. The proposed sparse model is tested using distorted three-phase signals from IEEE-1159-PQE database and the data generated from experimental laboratory setup. The analysis of absolute and mean square error is presented to validate the performance of the proposed model.**

***Index Terms*—Sequence component, Clarke transformation, H_∞ filter, state space model.**

I. Introduction

THE steady-state operation condition of the three-phase balanced power system is disrupted due to several reasons such as single-phase loading, unbalanced impedance of transmission lines and transformers, incomplete transposition of lines, lightning, line breaks, etc. Unbalance is considered as one of the PQ issues which can be measured through sequence components [1]. Due to the unbalanced situation of voltage across the phases, the system performance degrades and shortens the life of the equipment used in industry. Similarly, any deviation of system frequency from the normal value is a clear indicator of unbalanced condition between load and generation, which may lead to the grid failure by inadequate load shedding.

Therefore, the detection and subsequent mitigation of faults by designing protective equipment are crucial for a healthy power grid. To protect the grid, sequence components across all the phases and system frequency have to be estimated correctly. The amplitude and phase information of all the three phases in an unbalanced system can be extracted by analyzing the sequence components in terms of zero, positive, and negative sequence components. Adaptive filters are efficient to estimate the sequence components and frequency by modeling the three-phase voltage and current equations in a parametric form.

Several techniques have been proposed to estimate the symmetrical components and frequency from three-phase voltage and current signals. Discrete Fourier transform (DFT) is a popular nonparametric method used for frequency estimation, but this method suffers from inaccuracies due to the presence of system noise, inter- and intra-harmonics and spectral leakage [2], [3]. However, the errors due to the effect of spectral leakage and picket-fence are mitigated by modulated sliding discrete Fourier transform (msDFT) which is proposed for the measurement of harmonic and sequence components [4]. Reference [5] proposes an adaptive method using DFT and online algorithm, which is based on converting signal into phasor for symmetrical component estimation. Reference [6] also proposes a DFT-based technique for frequency estimation, which has good resistance to harmonics.

Artificial intelligence and soft computing techniques such as neural network, fuzzy logic, and genetic algorithm are quite popular for tracking PQ disturbances [7], [8]. These methods can track the signal parameters accurately with longer tracking time and slower convergence. Adaptive linear combiner structure is a single-layer model frequently used for harmonic and frequency estimation for single-phase power system [9]. However, the model based on multi-output can be used to track the symmetrical components of a three-phase system. Least mean square (LMS) is used for the up-

Manuscript received: July 12, 2018; accepted: October 12, 2019. Date of CrossCheck: October 12, 2019. Date of online publication: February 28, 2020.

The authors acknowledge the support of Indian Institute of Information Technology, Bhubaneswar, India, and Veer Surendra Sai University of Tecnology (Burla), Sambalpur, India, in terms of Laboratory and online Journal facilities to carry out this research work.

U. Subudhi and S. K. Mishra are with the Department of Electronics and Telecommunication Engineering, Indian Institute of Information Technology (IIIT), Bhubaneshwar, India (e-mail: umamani@iiit-bh.ac.in; sanjeev@iiit-bh.ac.in).

H. K. Sahoo (corresponding author) is with the Department of Electronics and Telecommunication Engineering, Veer Surendra Sai University of Tecnology (Burla), Sambalpur, India (e-mail: harish.86263@gmail.com).

DOI: 10.35833/MPCE.2018.000440

date of weight vector, which requires a proper choice of step size and the overall convergence rate is quite slow [10].

Compared to Kalman filter, extended Kalman filter (EKF) is an effective approach to estimate nonstationary PQ disturbances with increased noise level. Although EKF shows good estimation performance, it does not have stable convergence in the case of abrupt frequency change. Reference [11] proposes unscented Kalman filter (UKF) which is a derivative-free filter for the estimation of frequency in balanced and unbalanced power systems with the reduced complexity of computation [11]. However, the estimation accuracy of UKF is affected by the factors such as the divergence of estimation error due to some poorly-chosen initial conditions and the nature of noise. To overcome the above limitations, H_∞ filter is proposed, which is a robust form of Kalman filter to estimate the parameters of the sinusoid corrupted by white Gaussian noise [12], [13]. However, the filter performance is again restricted due to computation complexity and stable convergence for short-duration time-varying parameters.

The research work presented in this paper is based on a convex combination of H_∞ filters with the introduction of l_1 norm to the quadratic cost function for the estimation of both sequence components and frequency in an unbalanced three-phase power system. The proposed model is tested for wide categories of time-varying and short-duration PQ disturbances and the respective simulation results are presented.

The remainder of this paper is organized as follows. Section II explains the implementation steps of the H_∞ filter based on the sparse model. Section III and Section IV describe the state space models used to estimate the symmetrical components and frequency. Simulation results are presented in Section V to test and validate the proposed method considering different test cases such as frequency drift, harmonics, fault condition, etc. Section VI presents the conclusion of the results.

II. Filtering Algorithm of Sparse H_∞

In this proposed model, l_1 norm penalty is introduced to the quadratic cost function of H_∞ filter [14], [15]. The advantage of l_1 relaxation to the cost function lies in the extraction of the sparse solution compared to l_0 and l_2 norms with faster convergence. Moreover, in the case of Lasso regularized regression, if the budget used in the inequality is small enough, the solution vector is sparse but non-convex. In the case of higher order norms, the sparsity is lost which leads to more computation complexity [16]. The modified cost function with norm penalty J_k can be expressed as [17]:

$$J_k = \frac{1}{2}e_k^2 + \delta \|\boldsymbol{x}\|_1 \tag{1}$$

where $\|\cdot\|_1$ denotes the l_1 norm of a vector; e_k is the estimation error used in the cost function; $\boldsymbol{x}$ is the state vector; and δ is the weight assigned to the penalty term. Sparse H_∞ filter is based on two equations, namely, measurement equation and state equation which are given in (2)-(5) [12]. Measurement matrices and state transition matrices are generated using Taylor's series expansions of measurement and state equations. The information about measurement matrices and state matrices for sequence components, as well as frequency estimation, are provided in the subsequent sections.

$$\hat{\boldsymbol{y}}_{1,k/k} = \boldsymbol{H}_k \hat{\boldsymbol{x}}_{1,k/k} + v_k \tag{2}$$

$$\hat{\boldsymbol{y}}_{2,k/k} = \boldsymbol{H}_k \hat{\boldsymbol{x}}_{2,k/k} + v_k \tag{3}$$

$$\hat{\boldsymbol{x}}_{1,k+1/k} = f(\hat{\boldsymbol{x}}_{1,k/k}) + w_k \tag{4}$$

$$\hat{\boldsymbol{x}}_{2,k+1/k} = f(\hat{\boldsymbol{x}}_{2,k/k}) + w_k \tag{5}$$

where $\hat{\boldsymbol{y}}_{1,k/k}$ is the output vector generated through non-sparse filter estimation during the k^{th} instant using the predicted state vector of the k^{th} instant $\hat{\boldsymbol{x}}_{1,k/k}$; subscripts $1,k$ and $2,k$ are used to represent the convex combination using non-sparse and sparse adaptive filtering algorithms, respectively; $\boldsymbol{H}_k$ is the measurement matrix; v_k and w_k are the measurement noise and process noise, respectively, which are both white Gaussian noise process with zero mean; and $f(\cdot)$ is the supply frequency. As convex combination is formed using sparse and non-sparse adaptive filtering algorithms, $x_{1,k}$ and $y_{1,k}$ correspond to non-sparse adaptive filtering algorithm while $x_{2,k}$ and $y_{2,k}$ correspond to sparse adaptive filtering algorithm, respectively.

Two state update equations for convex combination are given in (6) and (7).

$$\hat{\boldsymbol{x}}_{1,k/k} = \hat{\boldsymbol{x}}_{1,k/k-1} + K_{1,k}(\boldsymbol{y}_k - \boldsymbol{H}_k \hat{\boldsymbol{x}}_{1,k/k-1}) \tag{6}$$

$$\hat{\boldsymbol{x}}_{2,k/k} = \hat{\boldsymbol{x}}_{2,k/k-1} - \rho \operatorname{sgn}(\hat{\boldsymbol{x}}_{2,k/k-1}) + K_{2,k}(\boldsymbol{y}_k - \boldsymbol{H}_k \hat{\boldsymbol{x}}_{2,k/k-1}) \tag{7}$$

where $K_{1,k}$ and $K_{2,k}$ are the Kalman gains of individual filtering algorithm which are time-varying parameters to control the weight adjustment in both the equations; and ρ is a value greater than 1. Similarly, the estimation error covariance update equations are given in (8) and (9).

$$\hat{\boldsymbol{p}}_{1,k+1/k} = \boldsymbol{F}_k \hat{\boldsymbol{p}}_{1,k/k-1} \boldsymbol{F}_k^{*\mathrm{T}} + \beta^2 \boldsymbol{G}_k \boldsymbol{G}_k^{\mathrm{T}} - \boldsymbol{F}_k \hat{\boldsymbol{p}}_{1,k/k-1} [\boldsymbol{H}_k^{*\mathrm{T}} \quad \boldsymbol{H}_k^{*\mathrm{T}}] \boldsymbol{R}_{e,k}^{-1} \begin{bmatrix} \boldsymbol{H}_k \\ \boldsymbol{H}_k \end{bmatrix} \hat{\boldsymbol{p}}_{1,k/k-1} \boldsymbol{F}_k^{*\mathrm{T}} + \boldsymbol{Q}_k \tag{8}$$

$$\hat{\boldsymbol{p}}_{2,k+1/k} = \boldsymbol{F}_k \hat{\boldsymbol{p}}_{2,k/k-1} \boldsymbol{F}_k^{*\mathrm{T}} + \beta^2 \boldsymbol{G}_k \boldsymbol{G}_k^{\mathrm{T}} - \boldsymbol{F}_k \hat{\boldsymbol{p}}_{2,k/k-1} [\boldsymbol{H}_k^{*\mathrm{T}} \quad \boldsymbol{H}_k^{*\mathrm{T}}] \boldsymbol{R}_{e,k}^{-1} \begin{bmatrix} \boldsymbol{H}_k \\ \boldsymbol{H}_k \end{bmatrix} \hat{\boldsymbol{p}}_{2,k/k-1} \boldsymbol{F}_k^{*\mathrm{T}} + \boldsymbol{Q}_k \tag{9}$$

where β is a constant between 0 and 1; $\boldsymbol{F}_k$ is the state transition matrix; $\hat{\boldsymbol{p}}_{1,k/k-1}$ and $\hat{\boldsymbol{p}}_{2,k/k-1}$ are the initial estimation error covariances used in update equation for filters 1 and 2, respectively; $\boldsymbol{Q}_k$ is the process noise covariance; $\boldsymbol{H}_k^*$ is the conjugate of the measurement matrix; $\boldsymbol{R}_{e,k}$ is the updated value of measurement covariance as shown in (10); and $\boldsymbol{G}_k = \boldsymbol{H}_k^{*\mathrm{T}}$.

$$\begin{cases} \boldsymbol{R}_{e,k} = \boldsymbol{R}_k + \begin{bmatrix} \boldsymbol{H}_k \\ \boldsymbol{H}_k \end{bmatrix} \hat{\boldsymbol{p}}_{1,k/k-1} [\boldsymbol{H}_k^{*\mathrm{T}} \quad \boldsymbol{H}_k^{*\mathrm{T}}] \\ \boldsymbol{R}_k = \begin{bmatrix} \boldsymbol{I} & \boldsymbol{0} \\ \boldsymbol{0} & -\gamma_f^2 \boldsymbol{I} \end{bmatrix} \end{cases} \tag{10}$$

where $\boldsymbol{R}_k$ is the initial value of measurement covariance; γ_f is the controlling parameter greater than 1; and $\boldsymbol{I}$ is the identity matrix. The net output across convex combination based sparse filtering algorithm is given as:

$$\hat{\boldsymbol{y}}_k = \lambda_k \hat{\boldsymbol{y}}_{1,k/k} + (1-\lambda_k) \hat{\boldsymbol{y}}_{2,k/k} \tag{11}$$

where $\lambda_k = sgm\, a_k = 1/(1+e^{-a_k})$. The role of the sigmoid function is to restrict the value of λ_k between 0 and 1 using a_k and reduce the gradient noise during error convergence [18].

III. Model of Symmetrical Component Estimation

Mathematically, unbalanced three-phase quantities are expressed in terms of symmetrical components as shown in (12) [10], [19]-[21].

$$\begin{cases} v_{ak} = V_0 \sin(\omega k T_s + \phi_0) + V_p \sin(\omega k T_s + \phi_p) + V_n \sin(\omega k T_s + \phi_n) \\ v_{bk} = V_0 \sin(\omega k T_s + \phi_0) + V_p \sin(\omega k T_s + \phi_p - 120°) + \\ \quad V_n \sin(\omega k T_s + \phi_n + 120°) \\ v_{ck} = V_0 \sin(\omega k T_s + \phi_0) + V_p \sin(\omega k T_s + \phi_p + 120°) + \\ \quad V_n \sin(\omega k T_s + \phi_n - 120°) \end{cases} \tag{12}$$

where V_{ak}, V_{bk}, V_{ck} are the voltage magnitudes of phases a, b, c, respectively; V_p, V_n, V_0 are the positive, negative, and zero sequence components and ϕ_p, ϕ_n, ϕ_0 are their respective phase angles, respectively; and ω, k, T_s are the angular frequency, discrete time instant and sampling time, respectively.

Using the equality, $\sin(A+B) = \sin A \cos A + \cos A \sin B$, (12) can be expanded as (13) and the discrete measurement equation used in state space model can be represented as (14).

$$\begin{cases} V_{ak} = V_0 \sin(\omega k T_s)\cos\phi_0 + V_0 \cos(\omega k T_s)\sin\phi_0 + \\ \quad V_p \sin(\omega k T_s)\cos\phi_p + V_p \cos(\omega k T_s)\sin\phi_p + \\ \quad V_n \sin(\omega k T_s)\cos\phi_n + V_n \cos(\omega k T_s)\sin\phi_n \\ V_{bk} = V_0 \sin(\omega k T_s)\cos\phi_0 + V_0 \cos(\omega k T_s)\sin\phi_0 + \\ \quad V_p \sin(\omega k T_s - 120°)\cos\phi_p + V_p \cos(\omega k T_s - \\ \quad 120°)\sin\phi_p + V_n \sin(\omega k T_s + 120°)\cos\phi_n + \\ \quad V_n \cos(\omega k T_s + 120°)\sin\phi_n \\ V_{ck} = V_0 \sin(\omega k T_s)\cos\phi_0 + V_0 \cos(\omega k T_s)\sin\phi_0 + \\ \quad V_p \sin(\omega k T_s + 120°)\cos\phi_p + V_p \cos(\omega k T_s + \\ \quad 120°)\sin\phi_p + V_n \sin(\omega k T_s - 120°)\cos\phi_n + \\ \quad V_n \cos(\omega k T_s - 120°)\sin\phi_n \end{cases} \tag{13}$$

$$\boldsymbol{y}_k = \boldsymbol{H}_k \boldsymbol{x}_k + \boldsymbol{v}_k \tag{14}$$

where $\boldsymbol{x}_k$ is the state vector. $\boldsymbol{v}_k$ must be included as the overall transmission of the power signal is always corrupted by noise.

By using the Taylor's series expansion measurement, $\boldsymbol{H}_k$ can be generated as given in (15) and the corresponding state vector $\boldsymbol{x}_k$ can be expressed in (16).

$$\boldsymbol{H}_k = \begin{bmatrix} \sin(\omega k T_s) & \cos(\omega k T_s) & \sin(\omega k T_s) & \cos(\omega k T_s) & \sin(\omega k T_s) & \cos(\omega k T_s) \\ \sin(\omega k T_s) & \cos(\omega k T_s) & \sin(\omega k T_s - 120°) & \cos(\omega k T_s - 120°) & \sin(\omega k T_s + 120°) & \cos(\omega k T_s + 120°) \\ \sin(\omega k T_s) & \cos(\omega k T_s) & \sin(\omega k T_s + 120°) & \cos(\omega k T_s + 120°) & \sin(\omega k T_s - 120°) & \cos(\omega k T_s - 120°) \end{bmatrix} \tag{15}$$

$$\boldsymbol{x}_k = \begin{bmatrix} V_0 \cos\phi_0 & V_0 \sin\phi_0 & V_p \cos\phi_p & V_p \sin\phi_p & V_n \sin\phi_n & V_n \sin\phi_n \end{bmatrix}^{\mathrm{T}} \tag{16}$$

The state equation for the above model is given by $\boldsymbol{x}_{k+1} = f(\boldsymbol{x}_k) + \boldsymbol{w}_k$, where $f(\boldsymbol{x}_k)$ is a functional mapping of state variable from the k^{th} instant to the $(k+1)^{\text{th}}$ instant and can be represented as given in (17). This functional mapping is required to generate a state transition matrix, which is a derivative based matrix obtained by using Taylor's series expansions. The amplitudes and phases of symmetrical components can be estimated by (18)-(23).

$$f(\boldsymbol{x}_k) = \begin{bmatrix} x_k(1) & x_k(2) & x_k(3) & x_k(4) & x_k(5) & x_k(6) \end{bmatrix} \tag{17}$$

$$\hat{V}_{0k} = \sqrt{\hat{x}_k^2(1) + \hat{x}_k^2(2)} \tag{18}$$

$$\hat{V}_{pk} = \sqrt{\hat{x}_k^2(3) + \hat{x}_k^2(4)} \tag{19}$$

$$\hat{V}_{nk} = \sqrt{\hat{x}_k^2(5) + \hat{x}_k^2(6)} \tag{20}$$

$$\hat{\phi}_{0k} = \arctan\frac{\hat{x}_k^2(2)}{\hat{x}_k^2(1)} \tag{21}$$

$$\hat{\phi}_{pk} = \arctan\frac{\hat{x}_k^2(4)}{\hat{x}_k^2(3)} \tag{22}$$

$$\hat{\phi}_{nk} = \arctan\frac{\hat{x}_k^2(6)}{\hat{x}_k^2(5)} \tag{23}$$

IV. Frequency Estimation Model

To develop an adaptive frequency estimation model, Clarke transformation is used to generate a complex phasor through $\alpha\beta$ components [22]-[24]. The discrete form of voltages across three phases of unbalanced system can be expressed as:

$$\begin{cases} v_{ak} = V_{ak} \sin(\omega k T_s + \theta) \\ v_{bk} = V_{bk} \sin(\omega k T_s + \theta - 2\pi/3) \\ v_{ck} = V_{ck} \sin(\omega k T_s + \theta + 2\pi/3) \end{cases} \tag{24}$$

where $\omega = 2\pi f$, f is the system frequency; and θ is the initial phase angle. Using Clarke transformation, $\alpha\beta$ components corresponding to (24) can be written mathematically as:

$$\begin{bmatrix} V_{ak} \\ V_{\beta k} \end{bmatrix} = \sqrt{\frac{2}{3}} \begin{bmatrix} 1 & -1/2 & -1/2 \\ 0 & \sqrt{3}/2 & -\sqrt{3}/2 \end{bmatrix} \begin{bmatrix} V_{ak} & V_{bk} & V_{ck} \end{bmatrix}^{\mathrm{T}} \tag{25}$$

The measured complex signal generated through $\alpha\beta$ components is corrupted by additive white Gaussian noise and can be expressed as [25]:

$$y_k = V_{ak} + \mathrm{j} V_{\beta k} = (A + \mathrm{j}B)\cos(\omega k T_s + \theta) + (B + \mathrm{j}C)\sin(\omega k T_s + \theta) + v_k \tag{26}$$

where $A = \sqrt{2/3}\, V_{ak} + (V_{bk} + V_{ck})/2\sqrt{6}$, $B = (V_{bk} - V_{ck})/2\sqrt{2}$, $C = \sqrt{3/2}\,(V_{bk} + V_{ck})/2$.

To model the complex phasor, measurement equation of sparse H_∞ filtering algorithm can be used as (14) where the corresponding measurement matrix is given by $\boldsymbol{H}_k = [0, 1]$. The state vector used in the estimation process is:

$$\boldsymbol{x}_k = \begin{bmatrix} x_k(1) & x_k(2) \end{bmatrix} \tag{27}$$

where $x_k(1)=e^{j\omega T_s}$; $x_k(2)=\alpha_k e^{j\omega k T_s+\phi_1}$; α_k is the magnitude; and ϕ_1 is the initial phase angle of the signal.

The functional mapping of state variable from the k^{th} instant to the $(k+1)^{th}$ instant is:

$$f(\boldsymbol{x}_k)=\begin{bmatrix}x_k(1) & x_k(1)x_k(2)\end{bmatrix} \tag{28}$$

The state transition matrix can be obtained from functional mapping by using Taylor's series expansion:

$$\boldsymbol{F}_k=\begin{bmatrix}1 & 0\\ x_k(2) & x_k(1)\end{bmatrix} \tag{29}$$

Thus, the frequency can be estimated from updated state variables by using the mathematical equation as:

$$\hat{f}_k=\mathrm{Im}\left(\frac{\log x_k(1)}{2\pi T_s}\right) \tag{30}$$

The state vector is updated by using the implementation steps of H_∞ filtering algorithm as given in Section II.

V. Simulation Results and Discussions

In the following analysis, different cases of unbalanced power signals are simulated and the corresponding comparison results are presented using sparse and non-sparse adaptive filtering algorithms including EKF, sparse EKF, H_∞ filtering algorithm and proposed sparse H_∞ filtering algorithm. For the simulation purpose, the controlling parameter δ and the parameter β in (8) are 0.98 and 0.10, respectively. The estimation error covariance matrix is also initialized as $\boldsymbol{P}_0=\rho\boldsymbol{I}$. The mixing parameter value λ_k is judiciously chosen between 0 and 1 to develop a convex combination. The response of the sparse H_∞ filtering algorithm is studied for different categories of PQ disturbances and comparison results are generated using MATLAB/Simulink.

A. Frequency Estimation of Three-phase Unbalanced Signals

For the purpose of simulation, three-phase voltage equations for a unbalanced system are considered as:

$$\begin{cases}v_{ak}=V_{ak}\cos(2\pi fkT_s+\theta)\\ v_{bk}=V_{bk}\cos(2\pi fkT_s+\theta-2\pi/3)\\ v_{ck}=V_{ck}\cos(2\pi fkT_s+\theta+2\pi/3)\end{cases} \tag{31}$$

The amplitudes of unbalanced three-phase signals are 1, 1.2 and 1.1 p.u. for phases *a*, *b*, and *c*, respectively. The signal frequency is chosen as 50 Hz. The complex phasor generated through $\alpha\beta$ transform is corrupted by white Gaussian noise of 30 dB signal noise ratio (SNR). The comparison is made to test the estimation accuracy between different adaptive filtering algorithms and the frequency estimation plot is shown in Fig. 1(a). Figure 1(b) represents a comparison of mean square estimation error between the filtering algorithms. The results indicate that the sparse model-based H_∞ filtering algorithm has a faster error convergence compared to other filtering algorithms.

Absolute frequency error is obtained by calculating the difference between the desired value and estimated filter output. Absolute frequency errors at different noise levels using different algorithms and the execution time are listed in Table I. Although EKF, sparse EKF and H_∞ filtering algorithms are capable of estimating frequency components, their performance deteriorates under high-noise conditions.

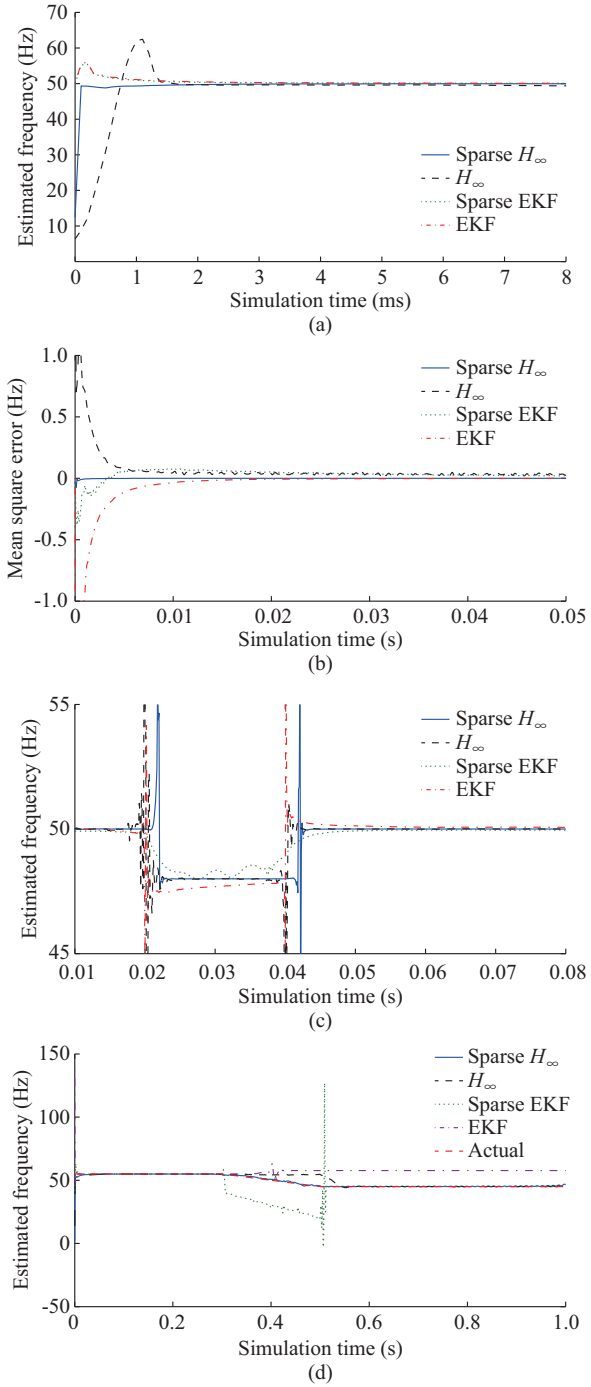

Fig. 1. Frequency estimation results. (a) Estimated frequency comparison. (b) Mean square error in frequency estimation. (c) Estimated frequency of power signal with step change in frequency. (d) Estimated frequency of power signal with ramp change in frequency.

A step change in frequency is introduced between 0.02 s and 0.04 s to the power signal of fundamental frequency of 50 Hz. In Fig. 1(c), it is observed that sparse H_∞ filtering algorithm tracks the frequency variation more accurately than other algorithms.

TABLE I
PERFORMANCE COMPARISON OF DIFFERENT ALGORITHMS

Algorithm	Frequency estimation error (Hz)			Execution time (ms)
	20 dB	30 dB	40 dB	
EKF	0.2020	0.151	0.0832	1.530
Sparse EKF	0.1425	0.107	0.0741	0.732
H_∞	0.0860	0.035	0.0120	0.596
Sparse H_∞	0.0310	0.008	0.0010	0.646

Further, a ramp change in frequency from 55 Hz to 45 Hz is considered between 0.3 s to 0.5 s and then the frequency remains constant at 45 Hz for the rest of the time in the unbalanced three-phase signal which is expressed in (31). It is observed that the proposed method is efficiently tracking the ramp change of signal with convergence time less than a half cycle and has good estimation accuracy as shown in Fig. 1(d). In the case of H_∞ filtering algorithm, the tracking starts beyond 0.3 s, i.e., around 0.48 s, which leads to the wrong result. Similarly, sparse EKF tracks the ramp variation from 40 Hz instead of 55 Hz, which is clearly visible from the figure.

B. Symmetrical Component Estimation of Unbalanced Signals

For the estimation of sequence components, the voltage signals for an unbalanced three-phase system are considered in (32). The estimation of zero, positive and negative sequence components are being carried out using state space modeling as explained in Section III.

$$\begin{cases} v_{ak} = 100\sin(\omega k T_s + 30°) \\ v_{bk} = 50\sin(\omega k T_s + 300°) \\ v_{ck} = 30\sin(\omega k T_s + 180°) \end{cases} \tag{32}$$

The steady-state errors for symmetrical components are shown in Fig. 2. It is observed from Fig. 2 that the convergence time of sparse H_∞ filter is less than 2.5 ms, which is the least.

Table II gives the absolute information of steady-state errors under different noise conditions. It is observed that the proposed model has lesser error value even under high-noise conditions such as 20 dB SNR.

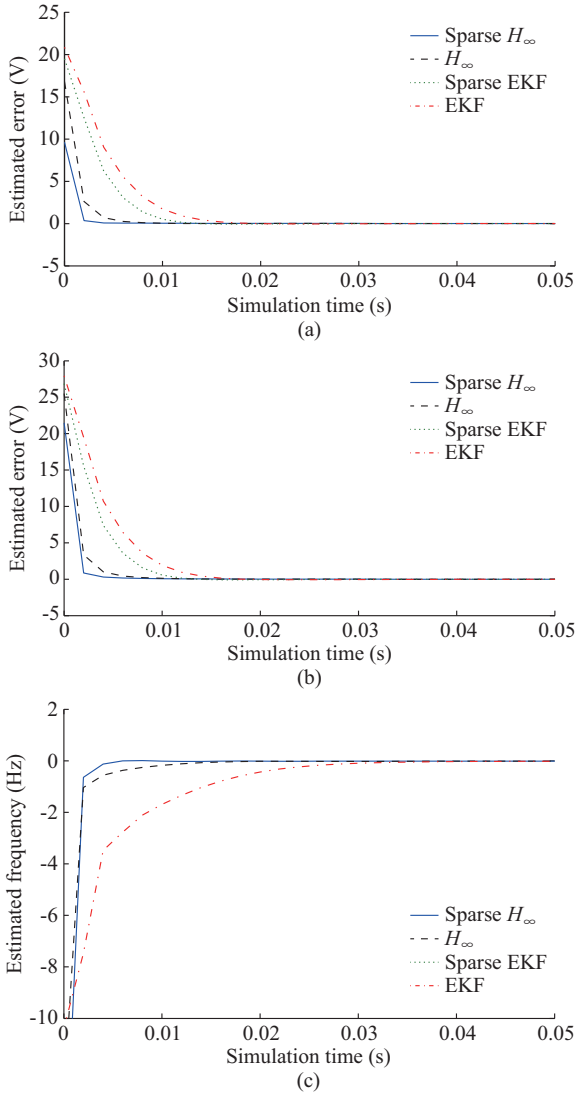

Fig. 2. Estimated steady-state errors. (a) Zero-sequence component. (b) Positive-sequence component. (c) Negative-sequence component.

TABLE II
ABSOLUTE STEADY-STATE ERROR

Algorithm	Zero-sequence estimation error (V)			Positive-sequence estimation error (V)			Negative-sequence estimation error (V)		
	20 dB	30 dB	40 dB	20 dB	30 dB	40 dB	20 dB	30 dB	40 dB
EKF	0.0140	0.0139	0.0089	0.0151	0.0055	0.00380	0.0162	0.0146	0.0144
Sparse EKF	0.0136	0.0092	0.0051	0.0046	0.0037	0.00210	0.0149	0.0118	0.0071
H_∞	0.0137	0.0109	0.0061	0.0087	0.0053	0.00230	0.0158	0.0121	0.0065
Sparse H_∞	0.0102	0.0032	0.0022	0.0033	0.0021	0.00018	0.0073	0.0035	0.0011

C. Symmetrical Component Estimation of Unbalanced Signals with Voltage Sag

The three-phase unbalanced signal is now considered with sag condition as shown in (32). The sag is introduced in a non-uniform manner from 0.050 s to 0.065 s across all the phases with 30% in phase *a*, 20% in phase *b* and 66% in phase *c*, respectively, which strictly follows IEEE standard (10%-90%).

In the case of zero--sequence and positive-sequence components, the disturbance caused by the sag is tracked with greater accuracy with the proposed sparse H_∞ filtering algorithm as shown in Fig. 3(a) and (b).

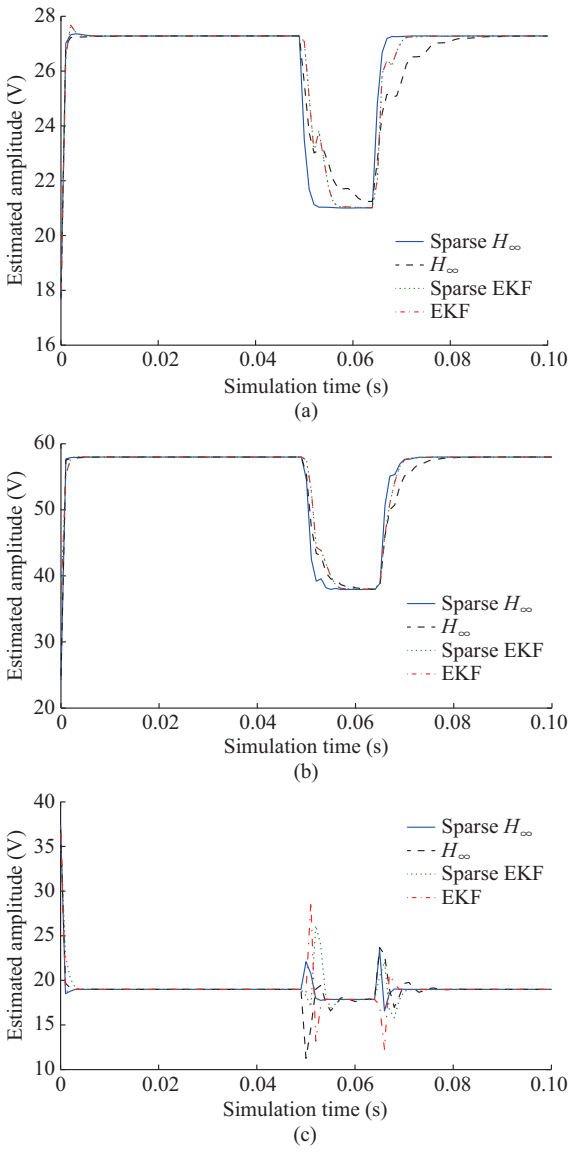

Fig. 3. Estimated amplitude. (a) Zero-sequence component. (b) Positive-sequence component. (c) Negative-sequence component.

The same has also been reflected through the estimation of negative-sequence components shown in Fig. 3(c), but the magnitude is less than the other two sequence components. In this case, the proposed algorithm has a superior performance.

D. Symmetrical Component Estimation of Harmonic Distorted Unbalanced Signals

The proposed model is tested considering unbalanced three-phase voltages which are contaminated with the 3rd harmonics. Its magnitudes equal to half those of the corresponding fundamental frequency components shown as:

$$\begin{cases} v_{ak} = 100\sin(\omega k T_s + 30°) + 50\sin(\omega k T_s + 20°) \\ v_{bk} = 50\sin(\omega k T_s + 300°) + 25\sin(\omega k T_s + 100°) \\ v_{ck} = 30\sin(\omega k T_s + 180°) + 15\sin(\omega k T_s + 70°) \end{cases} \tag{33}$$

Table III shows the estimated fundamental and third harmonic magnitudes along with their exact values. It is quite apparent from the results that the estimation errors lie in the range of 10^{-3}, whereas for other filters, the difference between the actual value and estimated value lies in the range of 10^{-2}. Also, it is observed from the results that the symmetrical components of fundamental and harmonics are estimated independently, i.e., the 3rd harmonics have no effect on the estimations.

E. Unbalanced Signal Estimation of Unbalanced Signals with Time-varying Amplitude

Three-phase unbalanced signals with time-varying amplitudes are taken into consideration in (34). The time variation in amplitudes is incorporated through slowly-varying sinusoidal components of frequency 1, 3 and 6 Hz, respectively.

$$\begin{cases} v_{ak} = A_1(kT_s)\sin(\omega k T_s + \pi/6) \\ v_{bk} = A_2(kT_s)\sin(\omega k T_s + \pi/3) \\ v_{ck} = A_3(kT_s)\sin(\omega k T_s + \pi) \end{cases} \tag{34}$$

$$\begin{cases} A_1(kT_s) = 0.15\sin(2\pi f_1 k T_s) + 0.05\sin(2\pi f_5 k T_s) \\ A_2(kT_s) = 0.05\sin(2\pi f_3 k T_s) + 0.02\sin(2\pi f_5 k T_s) \\ A_3(kT_s) = 0.025\sin(2\pi f_1 k T_s) + 0.005\sin(2\pi f_5 k T_s) \end{cases} \tag{35}$$

Comparison of estimated signals for three phases using different algorithms is shown in Fig. 4(a)-(c).

Though all algorithms track the time-varying signals, the proposed algorithm estimates the amplitude parameters more accurately than others. Mean square error plot is shown in Fig. 4(d). Average mean square error values of all phases for all algorithms are tabulated in Table IV. It is observed that mean square error is in the order of 10^{-7} with the proposed algorithm, which is much less than other algorithms.

TABLE III
SEQUENCE COMPONENTS ESTIMATION WITH HARMONICS

Algorithm	Fundamental amplitude (V)			The 3rd harmonic amplitude (V)		
	Zero-sequence	Positive-sequence	Negative-sequence	Zero-sequence	Positive-sequence	Negative-sequence
EKF	27.2774	57.9842	18.9857	24.4484	13.0195	18.6931
Sparse EKF	27.2759	57.9822	18.9832	24.4518	13.0145	18.6910
H_∞	27.2756	57.9802	18.9841	24.4533	13.0143	18.6908
Sparse H_∞	27.2828	57.9719	18.9845	24.4610	13.0100	18.6881
Actual	27.2926	57.9709	18.9872	24.4894	12.9682	18.6735

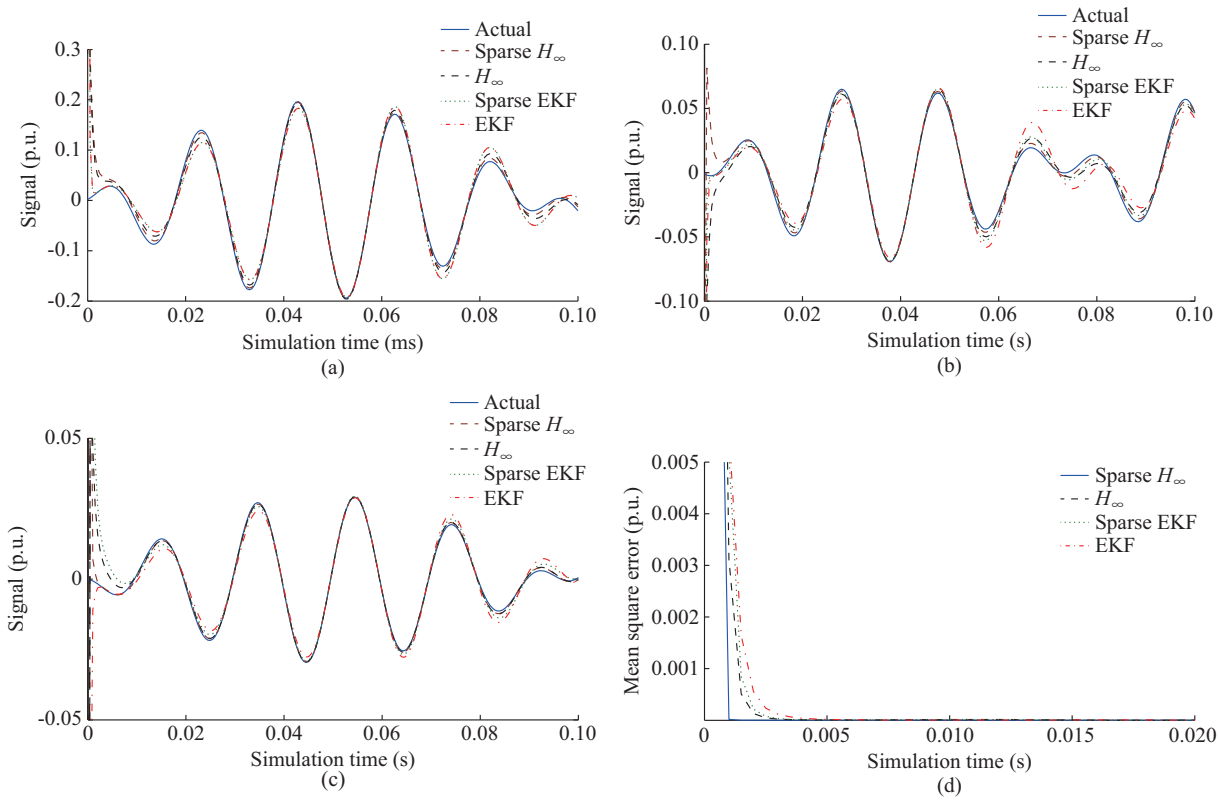

Fig. 4. Estimated signal and mean square error. (a) Phase *a*. (b) Phase *b*. (c) Phase *c*. (d) Mean square error.

TABLE IV
AVERAGE MEAN SQUARE ESTIMATION ERROR

Algorithm	Mean square estimation error (p.u)
EKF	1.06×10^{-2}
Sparse EKF	2.60×10^{-3}
H_∞	9.53×10^{-4}
Sparse H_∞	6.44×10^{-7}

F. Estimation of Unbalanced Signals with IEEE Database

Using IEEE-1159-PQE database, three-phase unbalanced signals are generated as shown in Fig. 5(a) [26]. For the purpose of testing, reconstructed signals obtained by all algorithms are compared with the original signals.

The respective comparison plots for the individual phases are shown in Fig. 5(b)-(d). Also, the mean square value of the difference between the desired response and estimated filter output is calculated and tabulated in Table V. In Table V, it is quite apparent that the proposed model convergence behavior has substantially improved.

G. Experimental Studies and Results

To validate the performance of the proposed algorithm for the estimation of harmonics, an experimental setup is taken as shown in Fig. 6 in the laboratory. The setup uses the voltage source inverter (VSI) with three-phase 180° conduction mode.

Unbalanced resistive loads of 100 W, 40 W, 200 W are connected to phases *a*, *b*, and *c*, respectively. The specifications of the system are: ① DC supply: 75 V; ② inverter: three-phase, 180° mode VSI (Frax); ③ load: 100W , 40 W, 200 W; ④ digital storage oscilloscope: 100 MHz, sample rate 50 ks/s, four channels, personal computer (PC) connectivity-universal serial bus port; ⑤ PC: 2.4 GHz, 2 GB RAM.

The load voltage waveforms are stored in a digital storage oscilloscope (Gwinstek) across the load resistors and then acquired data are transferred to PC through communication software.

Figure 7 represents the signal generated in all three phases of the experimental setup. Figure 8 shows the estimation of voltage signals across all the phases employing different algorithms using the data obtained from the setup. It is observed that the proposed algorithm estimates very close to the actual signal than other algorithms.

The performance of the algorithms which gives the accuracy of estimation is estimated by:

$$p=\frac{\sum_{k=1}^{N}(y_k-\hat{y}_k)^2}{\sum_{k=1}^{N}\hat{y}_k^2}\times 100\% \tag{35}$$

The less the value of p, the more is the estimation accuracy. The performance of the algorithms is shown in Table VI.

Along with the above performance index, the mean square estimation error is also calculated to validate the performance of the proposed model in Table VII. It is seen from the values that the proposed method achieves more significant estimation accuracy than others.

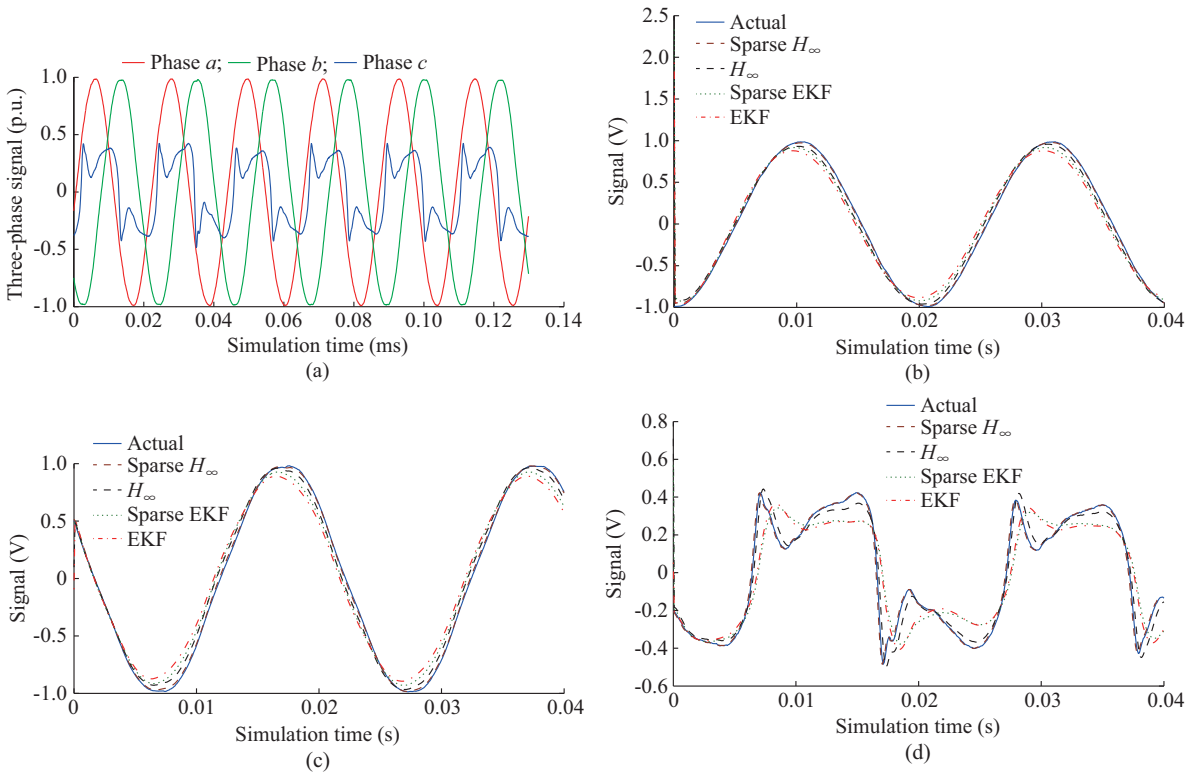

Fig. 5. Signals. (a) From IEEE database. (b) Estimated in phase *a*. (c) Estimated in phase *b*. (d) Estimated in phase *c*.

TABLE V
MEAN SQUARE ESTIMATION ERROR OF SIGNALS IN DIFFERENT PHASES

Algorithm	Mean square estimation error (p.u.)		
	Phase *a*	Phase *b*	Phase *c*
EKF	2.5000×10^{-3}	1.3000×10^{-3}	2.4000×10^{-3}
Sparse EKF	1.1000×10^{-3}	3.3031×10^{-3}	5.2126×10^{-3}
H_∞	9.4723×10^{-6}	6.5344×10^{-5}	5.3988×10^{-5}
Sparse H_∞	2.4672×10^{-8}	4.0371×10^{-7}	5.0840×10^{-7}

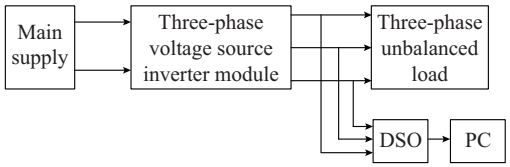

Fig. 6. Experimental setup for real data generation.

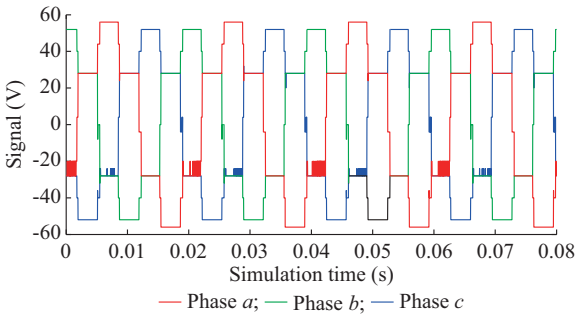

Fig. 7. Signal generated from experimental setup.

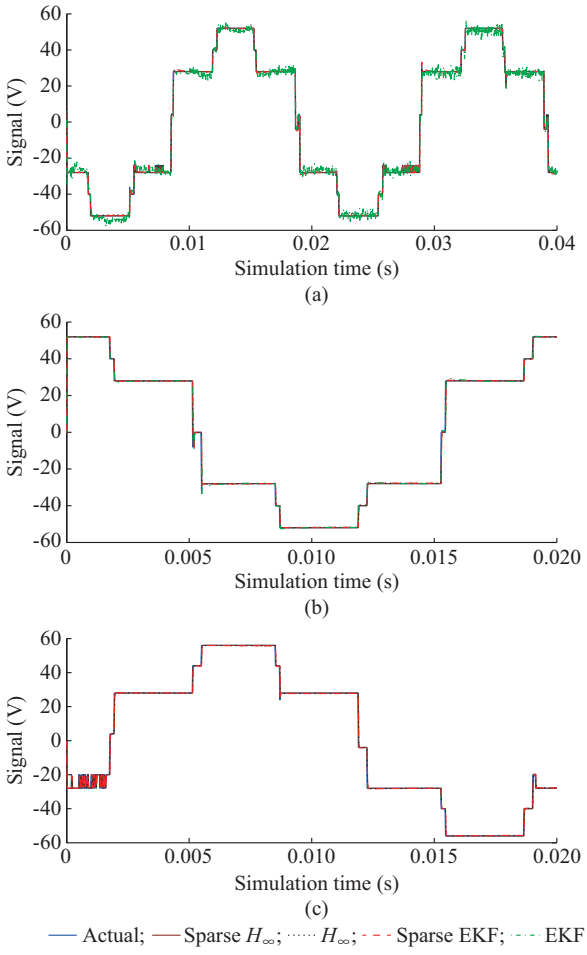

Fig. 8. Estimation of voltage signals. (a) Phase *a*. (b) Phase *b*. (c) Phase *c*.

TABLE VI
COMPARISON OF PERFORMANCE INDICES OF PRACTICAL DATA

Algorithm	Parameter p
EKF	1.5900
Sparse EKF	0.3200
H_∞	0.0301
Sparse H_∞	0.0118

TABLE VII
MEAN SQUARE ESTIMATION ERROR

Algorithm	Mean square estimation error (p.u.)		
	Phase a	Phase b	Phase c
EKF	6.2130×10^{-4}	1.196×10^{-5}	1.2443×10^{-4}
Sparse EKF	3.0234×10^{-6}	1.357×10^{-6}	1.5700×10^{-5}
H_∞	1.9262×10^{-7}	1.710×10^{-7}	2.3300×10^{-7}
Sparse H_∞	2.1630×10^{-9}	1.710×10^{-7}	8.9829×10^{-9}

VI. CONCLUSION

The proposed sparse model is tested using three-phase unbalanced voltages to estimate sequence components and frequency similar to practical systems. The estimation error is bounded due to norm penalty introduced in the cost function. The most important advantage of this method lies in developing a general-purpose processing unit for three-phase unbalanced conditions with less computation burden. The proposed model is also able to resolve the three-phase voltages in terms of sequence components and the estimated parameters across all the phases can provide accurate information about the dominant harmonics presenting in three-phase power system. With the proper knowledge about the order of harmonics, harmonic elimination filter can be designed for power system protection.

REFERENCES

[1] *IEEE Recommended Practice for Monitoring Electric Power Quality Industrial and Commercial Applications*, IEEE Standard 1159, 2009.

[2] M. M. Begovic, P. M. Djuric, S. Dunlap *et al*., "Frequency tracking in power networks in the presence of harmonics," *IEEE Transactions on Power Delivery*, vol. 8, no. 2, pp. 480-486, Apr. 1993.

[3] J. Z. Yang and C. W. Liu, "A precise calculation of power system frequency," *IEEE Transactions on Power Delivery*, vol. 16, no. 3, pp. 361-366, Jul. 2001.

[4] I. Carugati, C. M. Orallo, P. G. Donato *et al*., "Three-phase harmonic and sequence components measurement method based on msdft and variable sampling period technique," *IEEE Transactions on Instrumentation and Measurement*, vol. 65, no. 8, pp. 1761-1772, Aug. 2016.

[5] R. Naidoo, P. Pillay, J. Visser *et al*., "An adaptive method of symmetrical component estimation," *Electric Power Systems Research*, vol. 158, pp. 45-55, Mar. 2018.

[6] H. Xue, M. Wang, R. Yang *et al*., "Power system frequency estimation method in the presence of harmonics," *IEEE Transactions on Instrumentation and Measurement*, vol. 65, no. 1, pp. 56-69, Jan. 2016.

[7] R. P. M. Silva, A. C. B. Delbem, and D. V. Coury, "Genetic algorithms applied to phasor estimation and frequency tracking in PMU development," *International Journal of Electrical Power & Energy Systems*, vol. 44, no. 1, pp. 921-929, Jan. 2013.

[8] M. Badoni, A. Singh, and B. Singh, "Adaptive neurofuzzy inference system least-mean-square-based control algorithm for dstatcom," *IEEE Transactions on Industrial Informatics*, vol. 12, no. 2, pp. 483-492, Apr. 2016.

[9] M. Joorabian, S. Mortazavi, and A. Khayyami, "Harmonic estimation in a power system using a novel hybrid least squares-adaline algorithm," *Electric Power Systems Research*, vol. 79, no. 1, pp. 107-116, Jan. 2009.

[10] M. I. Marei, E. F. El-Saadany, and M. M. Salama, "A processing unit for symmetrical components and harmonics estimation based on a new adaptive linear combiner structure," *IEEE Transactions on Power Delivery*, vol. 19, no. 3, pp. 1245-1252, Jul. 2004.

[11] C. Wu, M. E. Magaña, and E. CotillaSánchez, "Dynamic frequency and amplitude estimation for three-phase unbalanced power systems using the unscented kalman filter," *IEEE Transactions on Instrumentation and Measurement*, vol. 68, no. 9, pp. 3397-3395, Sept. 2019.

[12] K. Nishiyama, "Robust estimation of a single complex sinusoid in white noise - H_∞ filtering approach," *IEEE Transactions on Signal Processing*, vol. 47, no. 10, pp. 2853-2856, Oct. 1999.

[13] H. Sahoo, P. Dash, and N. Rath, "Frequency estimation of distorted non-stationary signals using complex H_∞ filter," *AEU-International Journal of Electronics and Communications*, vol. 66, no. 4, pp. 267-274, Apr. 2012.

[14] Y. Chen, H. C. So, and W. Sun, "l_p-norm based iterative adaptive approach for robust spectral analysis," *Signal Processing*, vol. 94, pp. 144-148, Jan. 2014.

[15] K. Shi and P. Shi, "Convergence analysis of sparse lms algorithms with l_1-norm penalty based on white input signal," *Signal Processing*, vol. 90, no. 12, pp. 3289-3293, Dec. 2010.

[16] T. Hastie, R. Tibshirani, and M. Wainwright, *Statistical Learning with Sparsity: the Lasso and Generalizations*. Boca Raton, USA: CRC Press, 2015.

[17] Y. Chen, Y. Gu, and A. O. Hero, "Sparse LMS for system identification," in *Proceedings of IEEE International Conference on Acoustics, Speech and Signal Processing*, Taipei, China, Apr. 2009, pp. 3125-3128.

[18] J. Arenas-García, A. R. Figueiras-Vidal, and A. H. Sayed, "Mean-square performance of a convex combination of two adaptive filters," *IEEE Transactions on Signal Processing*, vol. 54, no. 3, pp. 1078-1090, Mar. 2006.

[19] R. Kumar, B. Singh, and D. Shahani, "Symmetrical components-based modified technique for power-quality disturbances detection and classifi cation," *IEEE Transactions on Industry Applications*, vol. 52, no. 4, pp. 3443-3450, Jul. 2016.

[20] D. Yazdani, M. Mojiri, A. Bakhshai *et al*., "A fast and accurate synchronization technique for extraction of symmetrical components," *IEEE Transactions on Power Electronics*, vol. 24, no. 3, pp. 674-684, Mar. 2009.

[21] U. Subudhi, H. K. Sahoo, and S. K. Mishra, "Harmonics and decaying DC estimation using volterra LMS/F algorithm," *IEEE Transactions on Industry Applications*, vol. 54, no. 2, pp. 1108-1118, Mar. 2018.

[22] A. Rastegarnia, A. Khalili, V. Vahidpour *et al*., "Frequency estimation of unbalanced three-phase power systems using the modified adaptive filtering," *American Journal of Signal Processing*, vol. 5, no. 2A, pp. 16-25, Aug. 2015.

[23] Y. Chen and H. C. So, "Accurate parameter estimation for unbalanced three-phase system," *The Scientific World Journal.* doi: 10.1155/2014/539420.

[24] P. Dash, K. Krishnanand, and R. Patnaik, "Dynamic phasor and frequency estimation of time-varying power system signals," *International Journal of Electrical Power & Energy Systems*, vol. 44, no. 1, pp. 971-980, Jan. 2013.

[25] R. Arablouei, K. Doğçancay, and S. Werner, "Adaptive frequency estimation of three-phase power systems," *Signal Processing*, vol. 109, pp. 290-300, Apr. 2015.

[26] *Power Quality Event Characterization*, IEEE Power Quality Standard 1159.2, 2003/

Umamani Subudhi received the M.Tech. degree from the Kalinga Institute of Industrial Technology University, Bhubaneswar, India, in 2008. She is currently working toward the Ph.D. degree with the International Institute of Information Technology (IIIT) Bhubaneswar, Bhubaneswar, India. She is currently working as an Assistant Professor in the Department of Electrical Engineering at IIIT Bhubaneswar, Bhubaneswar, India. She is a Life Member of Indian Society for Technical Education (ISTE) and Member of IEEE. Her research interests include power quality estimation, adaptive filtering, and power electronics.

Harish Kumar Sahoo received the B.E. degree from Utkal University, Bhu-

baneswar, India, in 1997, the M. Tech. degree in electronics systems and communication engineering from the National Institute of Technology, Rourkela, India, in 2005, and the Ph. D. degree in engineering from Sambalpur University, Sambalpur, India, in 2014. He served as Assistant Professor in IIIT Bhubaneswar, Bhubaneswar, India, from 2010 to 2016. He is currently an Associate Professor with the Department of Electronics and Telecommunication Engineering, Veer Suredra Sai University of Technology, Sambalpur, India. He has authored and coauthored 28 research papers in international journals and conferences of IEEE, Elsevier and other reputed publishers. He is a Life Member of the Indian Society for Technical Education. He is an active reviewer of journal papers for IEEE Transactions, IET, Elsevier, and Springer. His research interests include adaptive filtering and soft computing applications in the area of wireless communication and power quality.

Sanjeev Kumar Mishra received the B.E. and M. Tech degrees in electronics and communication engineering from the Utkal University, Bhubaneswar, India, and the Ph. D. degree in electrical engineering from Indian Institute of Technology (IIT) Bombay, Mumbai, India, in 2012. He is currently working as an Assistant Professor in the Department of Electronics and Telecommunication Engineering at IIIT Bhubaneswar, Bhubaneswar, India. He has published more than 90 papers in IEEE, PIER, MOTL, IJACSP, JMPCE, IJRFMCAE international and IETE, CSIR-IJRSP, CSIR IJAP national journals and conferences. His research work has been cited in more than 500 journal papers. He has written a book and filed 2 patents in the field of antennas. His research interests include radio frequency and microwave circuits and system design, planar antennas design, radar systems, wireless communication, and microwave measurements.